

# Giant electro-thermal conductivity and spin-phonon coupling in an antiferromagnetic oxide

C. Chiorescu,<sup>1</sup> J. J. Neumeier,<sup>2</sup> and J. L. Cohn<sup>1</sup>

<sup>1</sup>*Department of Physics, University of Miami, Coral Gables, Florida 33124*

<sup>2</sup>*Department of Physics, Montana State University, Bozeman, Montana 59717*

The application of weak electric fields ( $\lesssim 100$  V/cm) is found to dramatically enhance the lattice thermal conductivity of the antiferromagnetic (AF) insulator  $\text{CaMnO}_3$  over a broad range of temperature about the Néel ordering point (125 K). The effect is coincident with field-induced de-trapping of bound electrons, suggesting that phonon scattering associated with short- and long-ranged AF order is suppressed in the presence of the mobilized charge. This interplay between bound charge and spin-phonon coupling might allow for the reversible control of spin fluctuations using weak external fields.

PACS numbers: 66.70.-f, 75.47.Lx, 75.80.+q, 71.55.-i

The strong magneto-elastic coupling present in certain antiferromagnetic (AF) ferroelectrics [1] (e.g., hexagonal  $\text{YMnO}_3$ ) has attracted considerable attention recently because of its importance in mediating a coupling between magnetic and electric orders [2] and the potential of such multiferroics for applications [3]. The hexagonal manganites also possess very strong spin fluctuations characteristic of a spin liquid well above their Néel temperatures, possibly related to geometric spin frustration. This raises the prospect of manipulating *dynamic* magneto-elastic coupling in the paramagnetic phase (PM) of these or other compounds using external fields.

Dramatic signatures of such coupling in  $\text{YMnO}_3$  are a suppressed thermal conductivity [4] ( $\kappa$ ) and anomalous ultrasonic attenuation [5] over a broad temperature range in the PM phase. Two AF oxides with quite similar features in their thermal conductivities are the transition-metal monoxide,  $\text{MnO}$  [6] ( $T_N = 118$  K), and orthorhombic  $\text{CaMnO}_3$  [7, 8] ( $T_N \sim 125$  K). Like  $\text{YMnO}_3$ , both of these materials possess large exchange striction [9, 10] (with changes in lattice constants at  $T < T_N$ ,  $\Delta a/a \gtrsim 10^{-4}$ ), significant spin frustration [11, 12]  $\Theta/T_N \sim 4 - 5$  ( $\Theta$  is the Curie-Weiss temperature), and strong short-range spin correlations extending well above  $T_N$  [11, 13]. The suppressed thermal conductivities in the PM phase of  $\text{YMnO}_3$  and  $\text{CaMnO}_3$  (and by extension,  $\text{MnO}$ ) have been proposed to arise from the scattering of acoustic phonons by nanoscale strains generated by short-ranged spin correlations [4, 7]. This scattering diminishes rapidly when long range order is established, giving rise to sharp increases in  $\kappa$  at  $T < T_N$ .

$\text{CaMnO}_3$  is distinguished from  $\text{YMnO}_3$  and  $\text{MnO}$  by the presence of low-lying electron donor levels (oxygen vacancies) from which a small density of mobile electrons ( $\Delta n \sim 10^{16} \text{ cm}^{-3}$ ) can be released under relatively weak applied electric fields ( $F \lesssim 100$  V/cm) [14]. Here we demonstrate that these mobilized carriers are associated with a substantial reduction in phonon scattering, yielding relative changes in  $\kappa$  with field,  $(1/\kappa)(\Delta\kappa/\Delta F)$  that

are two orders of magnitude larger than found in quantum paraelectrics such as  $\text{KTaO}_3$  and  $\text{SrTiO}_3$  [15] where the field couples to soft-mode phonons. The apparent absence of permanent electric dipoles or lattice anomalies in  $\text{CaMnO}_3$  leads to the hypothesis that the mobilized electrons themselves mediate a suppression of phonon scattering from strain induced by short- and long-ranged magnetic order.

Measurements were performed on single-crystal and polycrystalline specimens of  $\text{CaMnO}_3$ . Their preparation methods and physical properties have been reported elsewhere [8, 14, 16, 17, 18]. We focus here on the crystal (dimensions  $2 \times 0.9 \times 0.05 \text{ mm}^3$ ) for which  $\kappa$  was measured for two different oxygen configurations produced by annealing at  $600^\circ \text{ C}$  in flowing oxygen and air, respectively. The net carrier density for the oxygen-annealed state, as determined from room-temperature Hall measurements [14], was  $N \simeq 6 \times 10^{18} \text{ cm}^{-3}$ . This corresponds to  $\sim 3 \times 10^{-4}$  electrons per formula unit, attributed to a very small oxygen deficiency. The carrier density after annealing in air is estimated [18] from the increase in room-temperature thermopower ( $-530 \mu\text{K}$  to  $-370 \mu\text{K}$ ) to be  $N \simeq 4 \times 10^{19} \text{ cm}^{-3}$ .  $\kappa$  was measured with a steady-state technique employing a heater and  $25 \mu\text{m}$ -diameter chromel-constantan thermocouple; four-probe electrical resistivity ( $\rho$ ) was measured during the same experiments.  $\kappa(I, T)$  was measured for the air-annealed crystal in the presence of *dc* transport currents ( $I = 5 \text{ nA} - 10 \text{ mA}$ ). With the specimen suspended in vacuum and thermally anchored at only one end, Joule heating was significant at the highest currents. The average specimen temperature (relative to a resistance sensor mounted on the cold stage) was monitored with a second thermocouple following application of a transport current, and allowed to stabilize prior to energizing the specimen heater for determining  $\kappa$ . Linearity in the heater power -  $\Delta T$  response was confirmed at various temperatures throughout the measurement range.

Figure 1 (lower panel) shows  $\kappa(T)$  after oxygen (dashed curve) and air (circles) annealing. The  $I = 0$  and

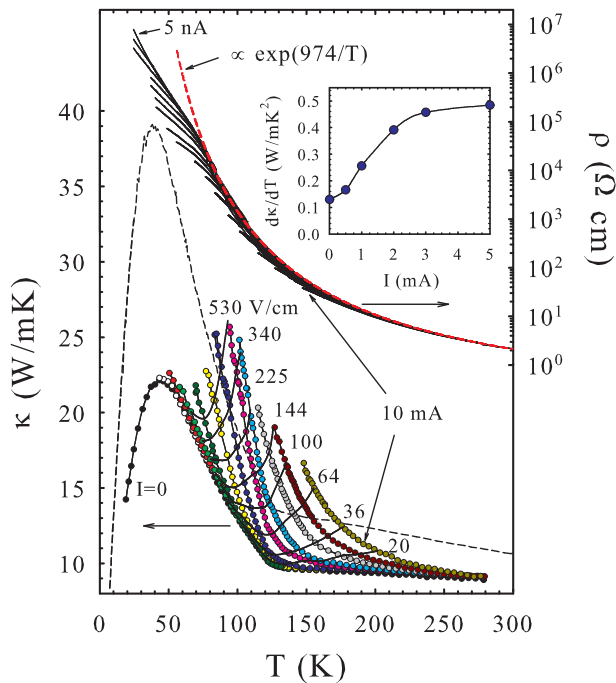


FIG. 1: (Color online) Lower panel (left ordinate):  $\kappa(T)$  for the air-annealed  $\text{CaMnO}_3$  crystal (circles) at various transport currents, from right to left (in mA): 10, 5, 3, 2, 1, 0.5, 0.25, 0.1, 0.05, 0.01, 0. The solid curves bridging  $\kappa(T)$  plots are contours of constant electric field (values labeled). The dashed curve represents data for the oxygen-annealed crystal for  $I = 0$ . Upper panel (right ordinate):  $\rho(T)$  for the same currents as  $\kappa(T)$  as well as the following (in  $\mu\text{A}$ ): 5, 3, 1, 0.3, 0.1, 0.03, 0.01, 0.005. Inset: current dependence of the slope,  $d\kappa/dT$ , for air annealing.

$I = 10$  mA plots for air annealing are labeled. Constant electric field ( $F$ ) contours (with values labeled) are represented by solid curves bridging the constant current plots. These fields,  $F = \rho J$ , were determined from  $\rho(T)$  data (upper panel). The abrupt upturn in  $\kappa$  upon entering the AF ordered phase is evident near  $T_N \approx 120$  K. Note that for the  $I = 0$  curves the slope just below  $T_N$ ,  $d\kappa/dT|_{T_N}$ , is greater for oxygen annealing, and increases with  $I$  for the air annealed crystal (inset, Fig. 1). These features are discussed further below. The data were reproducible upon thermal and current cycling, and after subsequent re-annealing.

Figure 2 (a) shows the  $T$ -dependence of the fractional change in thermal conductivity,  $(\Delta\kappa/\kappa) \equiv [\kappa(F, T) - \kappa(0, T)]/\kappa(0, T)$ , computed for these values of  $F$ . The enhancement of  $\kappa$  in field is substantial, approaching 100% for fields  $F > 100$  V/cm in the range  $80 \text{ K} < T < 130 \text{ K}$ , and becomes negligible at lower temperatures. Qualitatively similar results were found for the polycrystalline specimen, with a temperature interval for the largest field effects lower by about 50 K.

The field-enhanced  $\kappa$  correlates with an increased elec-

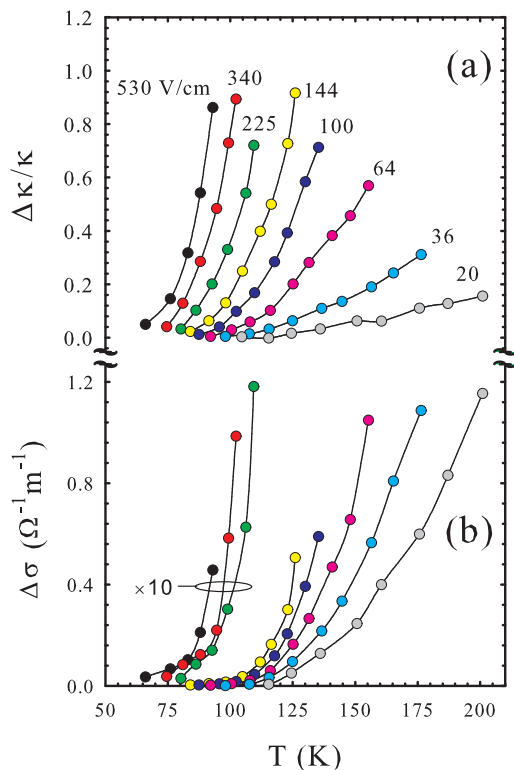


FIG. 2: (Color online) (a) Fractional change in thermal conductivity *vs* temperature at constant electric fields, (b) Field-induced change in electrical conductivity for the same field values as in (a).

trical conductivity,  $\Delta\sigma = \sigma(F, T) - \sigma(0, T)$  [Fig. 2 (b)]. As demonstrated by prior Hall effect studies on this same crystal [14], the mechanism underlying the increase in  $\sigma$  is Poole-Frenkel [20] release of carriers from Coulomb traps (oxygen vacancy donor levels) via field-assisted barrier-lowering. However, it is clear that the thermal conductivity of these mobilized electrons cannot account for the increase in  $\kappa$ . For example,  $\Delta\sigma \sim 0.5 \text{ } \Omega^{-1}\text{m}^{-1}$  at  $F = 144 \text{ V/cm}$  and  $T = 126 \text{ K}$ , corresponding to an increase in the electron density,  $\Delta n \simeq 3 \times 10^{16} \text{ cm}^{-3}$  (using a mobility [18]  $\sim 1 \text{ cm}^2/\text{V-s}$ ), about 50% of the equilibrium value at that temperature. The Wiedemann-Franz law, which provides an upper-bound estimate on the electronic thermal conductivity, yields  $\Delta\kappa_e = L_0\Delta\sigma T \simeq 1.5 \times 10^{-6} \text{ W/mK}$ , nearly seven orders of magnitude smaller than observed. Spin-wave heat conduction, though a possible contributor to  $\kappa$  at low  $T$  in the ordered phase, cannot account for  $\kappa$  well above  $T_N$ . Thus the increase of  $\kappa$  must have its origin in reduced phonon scattering.

Bound electrons may cause phonon scattering through static local distortions of bond lengths [21] or more extended, dynamic polaronic distortions, and possibly the diminution of this scattering as electrons become mobile in field explains the observations. But this proposal must be viewed as implausible given that the fraction of bound

electrons released is very small,  $\sim \Delta n/N \lesssim 10^{-3}$ , so that the density of such distortions is altered negligibly in field. Further supporting this view,  $\kappa$  at the highest  $F$  for the air-annealed crystal exceeds that in zero-field for the oxygen-annealed state (Fig. 1), in spite of the fact that the bound electron density in the former exceeds that of the latter by an order of magnitude. In addition, there is no evidence of permanent electric dipoles in this material [17, 22], the alignment of which in weak fields might conceivably alter the phonon scattering. This leads us to consider that the *mobilized* electrons themselves mediate a suppression of phonon scattering.

In order to assess how this might occur and to gain insight into the origin of the strong PM-phase phonon scattering, it is instructive to examine changes in structure induced by the onset of magnetic order. Anomalous Mn motion, stabilized at  $T < T_N$ , was recently proposed to explain the  $\kappa$  behavior of hexagonal YMnO<sub>3</sub> [23]. However, the unusual Mn-O bondlength changes [1] motivating this proposal are absent in the average and local structure of CaMnO<sub>3</sub> [24]. On the other hand, rotations of the MnO<sub>6</sub> octahedra couple strongly to the magnetic order in CaMnO<sub>3</sub> [13, 24] and provide a mechanism through which spin fluctuations at  $T > T_N$  may induce strain that scatters heat-carrying acoustic modes. Perturbations due to the polaronic motion [14, 18, 25] of mobilized electrons may compete with the distortions favored by short-ranged AF ordered domains.

Consider the scenario for phonon scattering by spin fluctuations introduced by Sharma *et al.* [4]. Strain fields associated with short-ranged AF spin-ordered regions have spatial extent given by the spin correlation length  $\xi$ . Slowly fluctuating on the timescale of lattice vibrations, they scatter acoustic phonons. For the case  $\lambda_p \ll \xi$  (where  $\lambda_p$  is the phonon wavelength [26]), their scattering rate can be approximated (for a spherical spin-correlated domain) as,  $\tau_{mag}^{-1} = p_0 v \pi (\xi/2)^2$  ( $p_0$  and  $v$  are the density of scatterers and phonon velocity, respectively). This scattering should be sharply diminished at  $T < T_N$  as long-range magnetic order is established. Residual strain in AF domain walls and other defects (e.g. twins) likely scatter phonons to low temperatures as evidenced by a phonon mean-free path [27],  $\ell_{ph} = 3\kappa/Cv$ , that remains  $< 1\mu\text{m}$  at the lowest measured  $T$ .

To examine this picture more quantitatively we employ the Debye-Calloway model [28] to compute the lattice thermal conductivity, adding  $\tau_{mag}^{-1}$  to a sum of traditional phonon scattering rates arising from other phonons (Umklapp), dislocations, and point-like defects [29]. We restrict our analysis to the PM phase and for simplicity ignore possible temperature dependencies of  $n_0$  and  $\xi$ , taking  $\gamma \equiv p_0 \pi (\xi/2)^2$  as a constant parameter for  $T > T_N$ . The  $I = 0$  data for air and oxygen annealing were first fitted by assuming the traditional phonon scattering terms to be independent of the annealing treat-

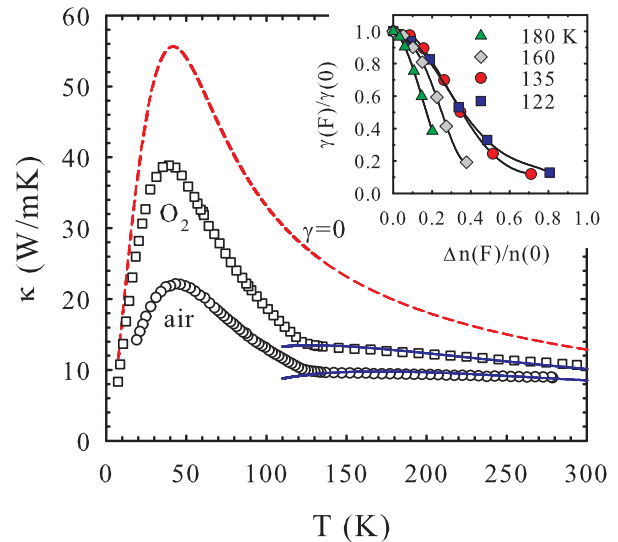


FIG. 3: (Color online) Comparison of calculated (curves) and measured (symbols)  $\kappa(T)$  for  $I = 0$ . The dashed curve is the computed  $\kappa$  in the absence of magnetic scattering ( $\gamma = 0$ ). The solid curves used  $\gamma = 2.51(0.82) \times 10^7 \text{ m}^{-1}$  for air (oxygen) annealing. Inset: magnetic scattering strength versus field-induced carrier density determined from fits to  $\kappa(F)$  at fixed  $T$ .

ment, and the computed  $\kappa$  in the absence of magnetic scattering ( $\gamma = 0$ ) was constrained to match the oxygen annealed data at the lowest  $T$  and to exceed the highest measured values (including those for air annealing in applied field) at intermediate  $T$ . Subsequently, the data for air annealing in applied field were fitted with  $\gamma$  as the only adjustable parameter.

Fig. 3 compares the calculated (solid curves) and measured  $\kappa(T)$ . Also shown is the hypothetical  $\kappa(T)$  in the absence of magnetic scattering ( $\gamma = 0$ , dashed curve). The values of  $\gamma = 2.51(0.82) \times 10^7 \text{ m}^{-1}$  for air (oxygen) annealing are similar to that employed for YMnO<sub>3</sub> [4]. For self-consistency, the distance between scatterers  $d = 2(3/4\pi n_0)^{1/3}$ , must be larger than their size  $\xi$ . Both YMnO<sub>3</sub> [4] and MnO [11] have comparable values of  $\xi \sim 20 - 50\text{\AA}$ . In the absence of a direct measurement of  $\xi$  for CaMnO<sub>3</sub>, taking  $\xi = 40\text{\AA}$  implies a density of scatterers  $p_0 = 2.0 \times 10^{18} \text{ cm}^{-3}$  for air annealing, or equivalently,  $d \simeq 100\text{\AA} > \xi$  as required.

Fitting the model to  $\kappa(F)$  at fixed  $T$  yields the decrease in magnetic scattering *vs.* the relative change in mobile carrier density (inset of Fig. 3). The decrease in  $\gamma$ , by up to a factor of 10 at the highest applied fields near  $T_N$ , implies a decrease in  $p_0$ ,  $\xi$  or both.

The nucleation of AF domains in the PM phase and their growth in the ordered phase likely depend on domain-wall pinning near lattice defects [30]. Mobilized electrons could reduce  $p_0$  by depinning AF domains, an idea motivated by comparing the zero-field data for air

and oxygen annealing. The larger  $\kappa$  and  $d\kappa/dT|_{T_N}$  observed for the more oxygenated crystal in the ordered phase (Fig. 1) suggests a coarsening of the domain structure, consistent with observations in  $\text{Gd}_2(\text{MoO}_4)_3$  of strong phonon scattering at ferroelastic domain boundaries [31]. Oxygen vacancies or their complexes are thus implicated in pinning (the estimate of  $p_0$  above suggests that  $\sim 10\%$  of vacancies participate in pinning).

The correlation between  $\kappa$  and  $d\kappa/dT|_{T_N}$  in applied electric field (Fig. 1) suggests that mobilized electrons cause depinning. The polaronic motion of charge carriers can increase the frequency of spin fluctuations [32], effectively reducing  $p_0$ . Regarding  $\xi$  there is precedent for its diminution by light charge-carrier doping in  $\text{Ca}_{1-x}\text{La}_x\text{MnO}_3$  [13] and  $\text{La}_{2-x}\text{Sr}_x\text{CuO}_4$  [32]. However, the carrier densities in these cases are several orders of magnitude larger than  $\Delta n$  induced by field in the present experiments. Both  $\kappa$  and  $d\kappa/dT|_{T_N}$  decrease with substitutional doping in  $\text{Ca}_{1-x}\text{La}_x\text{MnO}_3$  [8], contrary to the field-induced trend, but this may simply reflect the predominance of additional scattering from substitutional disorder. More direct measurements of the AF correlations in  $\text{CaMnO}_3$  as functions of temperature and applied electric field are clearly called for to further test and refine the ideas put forward here.

In summary, the present measurements of thermal conductivity in  $\text{CaMnO}_3$  imply that a small density of electrons released from donor states in weak electric fields substantially reduce the scattering of phonons associated with short- and long-ranged AF order. The results suggest that the correlated spin volume in the PM phase is highly sensitive to the injected carrier density and reversibly controlled by a transport current. Strong AF spin fluctuations, magnetostriction, and the presence of loosely-bound charges in defect states appear to be key ingredients underlying the observations. This novel manipulation of dynamic magneto-elastic coupling motivates further studies of spin correlations in this compound or others having similar characteristics.

This material is based upon work supported by the National Science Foundation under grants DMR-0072276 (Univ. Miami) and DMR-0504769 (Mont. St. Univ.), and the Research Corporation (Univ. Miami).

---

[1] S. Lee *et al.*, Nature **451**, 805 (2008); J. Cao *et al.*, Phys. Rev. Lett. **100**, 177205 (2008); D. Meier *et al.*, New J. Phys. **9**, 100 (2007); F. Ye *et al.*, Phys. Rev. B **73**, 220404(R) (2006).  
 [2] W. Eerenstein, N. D. Mathur, and J. F. Scott, Nature **442**, 759 (2006).  
 [3] M. Fiebig, J. Phys. D: Appl. Phys **38**, R123 (2005); T. Kimura *et al.*, Nature **426**, 55 (2003); N. Hur *et al.*, *ibid.* **429**, 392 (2004); T. Lottermoser *et al.*, *ibid.* **430**, 541 (2004).

[4] P. A. Sharma *et al.* Phys. Rev. Lett. **93**, 177202 (2004).  
 [5] M. Poirier *et al.*, Phys. Rev. B **76**, 174426 (2007).  
 [6] G. A. Slack and R. Newman, Phys. Rev. Lett. **1**, 359 (1958).  
 [7] J.-S. Zhou and J. B. Goodenough, Phys. Rev. B **66**, 052401 (2002).  
 [8] J. L. Cohn and J. J. Neumeier, Phys. Rev. B **66**, 100404(R) (2002).  
 [9] B. Morosin, Phys. Rev. B **1**, 236 (1970).  
 [10] Y. Moritomo *et al.*, Phys. Rev. B **64**, 214409 (2001).  
 [11] A. Renninger, S. C. Moss, and B. L. Averbach, Phys. Rev. **147**, 418 (1966); H. Betsuyaku, Sol. St. Commun. **26**, 345 (1977).  
 [12] J. J. Neumeier and D. H. Goodwin, J. Appl. Phys. **85**, 5591 (1999).  
 [13] E. Granado *et al.*, Phys. Rev. Lett. **86**, 5385 (2001).  
 [14] C. Chiorescu, J. L. Cohn, and J. J. Neumeier, B **76**, 020404(R) (2007).  
 [15] W. H. Huber, L. M. Hernandez, and A. M. Goldman, Phys. Rev. B **62**, 8588 (2000).  
 [16] J. J. Neumeier and J. L. Cohn, Phys. Rev. B **61** 14319 (2000).  
 [17] J. L. Cohn, M. Peterca, and J. J. Neumeier. Phys. Rev. B **70** 214433 (2004).  
 [18] J. L. Cohn, C. Chiorescu, and J. J. Neumeier, Phys. Rev. B **72**, 024422 (2005); C. Chiorescu, J. J. Neumeier, and J. L. Cohn, *ibid.* **73**, 014406 (2006).  
 [19] O. Chmaissem *et al.*, Phys. Rev. B **64**, 134412 (2001).  
 [20] J. Frenkel, Phys. Rev. **54**, 647 (1938).  
 [21] J. L. Cohn *et al.*, Phys. Rev. B **56**, R8495 (1997).  
 [22] A. Filippetti and N. A. Hill, Phys. Rev. B **65**, 195120 (2002).  
 [23] J.-S. Zhou *et al.*, Phys. Rev. B **74**, 014422 (2006).  
 [24] E. S. Bozin *et al.*, J. Phys. Chem. Sol. **69**, 2146 (2008).  
 [25] Y. R. Chen and P. B. Allen, Phys. Rev. B **64**, 064401 (2001); H. Meskine, T. Saha-Dasgupta, and S. Satpathy, Phys. Rev. Lett. **92**, 056401 (2004); H. Meskine and S. Satpathy, J. Phys.: Condens. Matter **17**, 1889 (2005).  
 [26] A reasonable estimate for thermal phonons is  $\lambda_p \sim hv/(3.8k_B T) \approx 2 - 6\text{\AA}$  in the PM phase.  
 [27] Specific heat ( $C$ ) data for  $\text{CaMnO}_3$  are reported by Y. Moritomo *et al.*, Phys. Rev. B **61**, 204409 (2001) and A. Cornelius *et al.*, *ibid.* **68**, 014403 (2003). The sound velocity  $v = 4,800$  m/s employed represents an average computed from the experimental Debye temperature ( $\Theta_D$ ).  
 [28] R. Berman, *Thermal Conduction in Solids* (Clarendon, Oxford, 1976).  
 [29] The scattering of phonons of frequency  $\omega = vq$  by other phonons (U-processes), dislocations, and point defects were represented by rates:  $A_1\omega^2 T \exp(-\Theta_D/bT)$ ,  $A_2\omega$ ,  $A_3\omega^4$ . Boundary scattering was found to be negligible in the measured temperature range. Parameter values (the same for air and oxygen annealing) were:  $A_1 = 2.63 \times 10^{-18}$  s  $\text{K}^{-1}$ ,  $A_2 = 7.65 \times 10^{-5}$ , and  $A_3 = 2.36 \times 10^{-43}$  s<sup>3</sup>. These values are comparable to those found for  $\text{YMnO}_3$  (Ref. 4).  $b$  was taken as 5 (Ref. 28).  
 [30] Yin-Yuan Li, Phys. Rev. **101**, 1450 (1956); B. K. Tanner, Contemp. Phys. **20**, 187 (1979).  
 [31] S. Mielcarek *et al.*, Proceedings of the 11th IEEE Int'l Symposium on Applications of Ferroelectrics, ISAF98, p. 415 (1998).  
 [32] V. Kataev *et al.*, J. Phys.: Condens. Matter **11**, 6571 (1999); K. Hirota *et al.*, Physica C 357-360, 61 (2001).